

Grid-based density functional calculations of many-electron systems

Amlan K. Roy*

*Department of Chemistry & Biochemistry,
University of California, Los Angeles, 90095, CA, USA*

Abstract

Exploratory variational pseudopotential density functional calculations are performed for the electronic properties of many-electron systems in the 3D cartesian coordinate grid (CCG). The atom-centered localized gaussian basis set, electronic density and the two-body potentials are set up in the 3D cubic box. The classical Hartree potential is calculated accurately and efficiently through a Fourier convolution technique. As a first step, simple local density functionals of homogeneous electron gas are used for the exchange-correlation potential, while Hay-Wadt-type effective core potentials are employed to eliminate the core electrons. No auxiliary basis set is invoked. Preliminary illustrative calculations on total energies, individual energy components, eigenvalues, potential energy curves, ionization energies, atomization energies of a set of 12 molecules show excellent agreement with the corresponding reference values of atom-centered grid as well as the grid-free calculation. Results for 3 atoms are also given. Combination of CCG and the convolution procedure used for classical Coulomb potential can provide reasonably accurate and reliable results for many-electron systems.

*Email: akroy@chem.ucla.edu. Present address: Department of Chemistry, University of Kansas, Lawrence, KS, 66045, USA.

I. INTRODUCTION

In the past few decades, density functional theory (DFT) [1, 2] based calculations have played a pivotal role in our understanding of the electronic structure, properties and dynamics of many-electron systems such as atoms, molecules and solids. This overwhelming success is chiefly due to their ability to offer accurate results and to account for the electron correlation effects in a transparent and tractable manner. Accordingly, a large number of elegant and efficient approaches are available today for the treatment of these systems covering a broad range of approximations, accuracy, computational and algorithmic schemes. Consequently, this has been a very fertile area of research in the recent years and continues to remain at the forefront of modern research.

Leaving aside a few attempts such as the high-order finite difference method [3], where without the explicit use of basis set, the discretized Kohn-Sham (KS) equation is directly solved on real-space grid, a vast majority of today’s all-electron or pseudopotential DFT methodologies instead employ some suitable basis set. Some of the notable ones include the plane waves (PW) or atom-centered localized basis sets such as Slater type orbitals (STO), Gaussian type orbitals (GTO), numerical radial functions, linear muffin-tin orbitals, etc. Among these, the GTO basis sets have gained more popularity over the others for nonperiodic systems such as molecules and clusters due to the convenient analytic routes they provide for the relevant matrix elements involving multiple centers. On a similar ground, PW basis sets are the preferred options for periodic systems. A gaussian and augmented-plane-wave DFT approach has also been reported [6, 7] where the KS molecular orbitals (MO) and the electronic charge densities are expanded in the gaussian basis and an augmented PW basis sets respectively.

Nowadays, linear combination of GTO based DFT calculations have become an invaluable and routine tool for quantum chemists, where the KS MOs are typically expanded in terms of the contracted gaussian functions centered on the atoms[4, 5]. Furthermore, the electron density as well as the exchange-correlation (XC) potentials are also similarly expanded in terms of a finite number of *auxiliary* gaussian type basis functions. This obviates the necessity to compute the expensive four-centered integrals, making it an N^3 process.

In the *grid-based* methods, typically the multi-center molecular integrals are decomposed into monocentric atomic subintegrals using some weighting scheme and then each of these

latter are computed numerically on the respective atomic grid [8]. The radial integrals are performed through a variety of techniques, *viz.*, Gauss-Chebyshev quadrature of second kind [8], Chebyshev quadratures of first and second kind in conjunction with several mapping schemes [9], simple Gauss quadrature [10], transformation based on Euler-MacLaurin formula [11, 12], numerical quadratures [13], etc. Angular integrations often use the octahedral grid developed by Lebedev [14] or the Lobatto approaches [9]. Automatic numerical integrator generating an adaptive molecular grid depending on size and shell structure of the given basis set, has also been developed [15]. Recently, there has been interest in the real-space cartesian grid as well. For example in the Fourier Transform Coulomb method [16], molecular integrations are performed by dividing the gaussian shell pairs into “smooth” and “sharp” categories based on their exponents. Of late, a multiresolution technique, combining the atom-centered and cubic cartesian grid, with divided difference interpolation playing the role of a communicator between the two, have been shown to be quite efficient [17, 18].

In this article, we make a detailed systematic analysis of the performance and relevance of the cartesian coordinate grids (CCG) in the context of molecular DFT calculations. As our results in the following sections show, this is indeed capable of producing fairly accurate and physically meaningful results, at least for small molecules. We use the usual GTO-type linear expansion of the KS MOs; however no additional auxiliary basis set is utilized to express the charge density or the XC potential. The basis functions, the MOs, the electron density as well as the various two-electron potentials are directly set up in the 3D real CCG. The classical Hartree potential is obtained accurately and efficiently through a Fourier convolution method involving a set of FFT-inverse FFT pair [21, 22]. Analytical one-electron *ab initio* effective core potentials, consisting of a sum of gaussian functions are employed to represent the core electrons while energy-optimized truncated gaussian bases are chosen for the valence electrons. Here we restrict ourselves to the local density functionals of homogeneous electron gas to incorporate the XC effects, while more accurate, sophisticated functionals may be considered in future. The KS matrix eigenvalue equation is solved in the usual self consistent manner to obtain the KS orbitals and eigenvalues. Results are given for 12 representative molecules (5 diatomics and 7 polyatomics) and 3 atoms. In order to assess the accuracy and reliability, first we make a systematic investigation on the convergence of total energies, individual energy components and the integrated electron density, in various grid representation through a comparison with the reference theoretical

results. Then we compare the eigenvalues, atomization energies and the ionization energies with the literature data. Potential energy curves are given for two diatomics (HCl and Cl₂). The article is organized as follows: Section II gives the methods of computation. Section III presents a discussion on the results obtained while a few concluding remarks are made on the future and prospect in Section IV.

II. METHOD OF CALCULATION

We are interested in the single-particle KS equation for the ground state of a many-electron system under the influence of pseudopotential, which can be written as (atomic units employed unless otherwise stated),

$$\left[-\frac{1}{2}\nabla^2 + v_{ion}^p(\mathbf{r}) + v_H[\rho](\mathbf{r}) + v_{XC}[\rho](\mathbf{r}) \right] \psi_i(\mathbf{r}) = \epsilon_i \psi_i(\mathbf{r}) \quad (1)$$

where v_{ion}^p denotes the ionic pseudopotential for the system.

$$v_{ion}^p(\mathbf{r}) = \sum_{\mathbf{R}_a} v_{ion,a}^p(\mathbf{r} - \mathbf{R}_a) \quad (2)$$

with $v_{ion,a}^p$ signifying the ion-core pseudopotential associated with atom A , situated at \mathbf{R}_a . The Hartree potential $v_H[\rho](\mathbf{r})$ describes the classical electrostatic interactions among valence electrons while the XC potential $v_{XC}[\rho](\mathbf{r})$ represents the non-classical part of the Hamiltonian. $\{\psi_i^\sigma(\mathbf{r})\}, \sigma = \alpha$ or β , corresponds to a set of N occupied orthonormal MOs and the electronic density is given by the expression,

$$\rho(\mathbf{r}) = \rho^\alpha(\mathbf{r}) + \rho^\beta(\mathbf{r}) = \sum_i f_i^\alpha |\psi_i^\alpha(\mathbf{r})|^2 + \sum_i f_i^\beta |\psi_i^\beta(\mathbf{r})|^2 \quad (3)$$

where the f_i 's denote the occupation numbers.

The basis functions and the MOs are directly built on the real uniform 3D cartesian grid simulating a cubic box,

$$r_i = r_1 + (i - 1)h_r, \quad i = 1, 2, \dots, N_r; \quad \text{for } r \in \{x, y, z\} \quad (4)$$

where h_r and N_r denote the grid spacing and number of points in the grid respectively. The electron density in the grid is given by,

$$\rho(\mathbf{r}_g) = \sum_{\mu\nu} P_{\mu\nu} \chi_\mu(\mathbf{r}_g) \chi_\nu(\mathbf{r}_g) \quad (5)$$

where $P_{\mu\nu}$ signifies an element of the density matrix and the set $\{\chi_\mu(\mathbf{r})\}$ contains the contracted gaussian functions centered on the atoms. Any quantity including those in the above will be represented in the discretized grid with a subscript “g”.

The standard matrix form of the KS equation reads (for a system having K basis functions),

$$\mathbf{F}^{KS}\mathbf{C} = \mathbf{S}\mathbf{C}\epsilon \quad (6)$$

where \mathbf{C} is a $K \times K$ square matrix containing the expansion coefficients $C_{\mu i}$ and ϵ is the diagonal matrix of the orbital energies ϵ_i . \mathbf{S} corresponds to the overlap matrix and \mathbf{F}^{KS} denotes the total KS matrix including the core Hamiltonian and the effective KS potential,

$$F_{\mu\nu}^{KS} = \int \chi_\mu(\mathbf{r}) [h^{core} + v_{HXC}(\mathbf{r})] \chi_\nu(\mathbf{r}) d\mathbf{r} = H_{\mu\nu}^{core} + \langle \chi_\mu(\mathbf{r}) | v_{HXC}(\mathbf{r}) | \chi_\nu(\mathbf{r}) \rangle \quad (7)$$

The first term in the right hand side accounts for the one-electron energies in the Hamiltonian. The overlap, kinetic and nuclear-electron attraction integrals are identical to those obtained in the gaussian basis-set based HF methods and we have used the standard recursion algorithms [23, 24] for their evaluation. Significant progress has been made in the development of rigorous *ab initio* effective core potentials and in this work we employ the angular-momentum dependent form as proposed by [25, 26]. While construction of the pseudopotential matrix elements in gaussian basis sets is currently in progress, in the present implementation, they are imported from the widely used quantum chemistry program GAMESS output (with printing option 3)[27].

For finite systems, the simplest and perhaps the most crude way to calculate v_H is by direct numerical integration, which is feasible for only small systems. However the most widely used approach is to solve the corresponding Poisson equation. Recently however, in the literature, the conventional *Fourier convolution* method and some of its variants have been shown to be quite accurate and efficient in the context of molecular modeling. In particular, here we adopt the approach as put forth in [21, 22].

$$\begin{aligned} \rho(\mathbf{k}_g) &= \text{FFT}\{\rho(\mathbf{r}_g)\} \\ v_H(\mathbf{r}_g) &= \text{FFT}^{-1}\{v_H^c(\mathbf{k}_g) \rho(\mathbf{k}_g)\} \end{aligned} \quad (8)$$

Here $\rho(\mathbf{k}_g)$ and $v_H^c(\mathbf{k}_g)$ denote the Fourier integrals of density and the Coulomb interaction kernel in the grid. It may be noted that while $\rho(\mathbf{k}_g)$ can be easily obtained from the discrete Fourier transform of its real-space values by standard FFT, the calculation of the latter is

nontrivial and requires caution due to the presence of singularity in the real space. This is tackled by decomposing the kernel into long- and short-range terms:

$$v_H^c(\mathbf{r}_g) = \frac{\text{erf}(\alpha r)}{r} + \frac{\text{erfc}(\alpha r)}{r} \equiv v_{H_{long}}^c(\mathbf{r}_g) + v_{H_{short}}^c(\mathbf{r}_g) \quad (9)$$

where $\text{erf}(x)$ and $\text{erfc}(x)$ denote the error function and its complements respectively. The Fourier integral of the short-range part is calculated analytically whereas the long-range interaction is directly obtained from the FFT of the real-space values. It may be mentioned that while the above FFT-based Ewald type summation method scales as $N \ln N$, two other Poisson-solvers have gained popularity in the context of large-scale electronic structure calculation within the KS DFT framework, which are quite efficient and scale *linearly*. In the fast multipole method (FMM) type approaches, the near-field contributions are tackled explicitly, whereas the far-field is treated through a clustering of the spatial cells and representing the field with a multipole expansion. Another route employs the highly efficient multigrid method within the real-space formalism such as a finite-difference or finite-element scheme. A review of the various available techniques could be found in [28].

One of the most critical issues in any DFT calculation is the choice of appropriate XC functionals, the exact form of which is unknown as yet and must be approximated. In the literature, an enormous number of functionals with varying complexity, property and accuracy have been published; the present work employs the simple local XC functionals of a homogeneous electron gas (formula V of ref. [29]). In the absence of any analytical method, the corresponding two-electron matrix elements can be either calculated numerically on the grid or be fitted by an auxiliary set of gaussian functions as suggested by [30, 31] and employed in some of the existing DFT codes [4, 5]. This work employs the direct numerical integration on the CCG to obtain these matrix elements, *viz.*,

$$\langle \chi_\mu(\mathbf{r}_g) | v_{HXC}(\mathbf{r}_g) | \chi_\nu(\mathbf{r}_g) \rangle = h_x h_y h_z \sum_g \chi_\mu(\mathbf{r}_g) v_{HXC}(\mathbf{r}_g) \chi_\nu(\mathbf{r}_g) \quad (10)$$

The algebraic eigenvalue equation is solved in the usual self-consistent manner and the total energy of the system can be obtained as a sum of the various components in the standard way. Three convergence criteria were imposed in this work *viz.*, (i) the electronic energy differences between two successive iterations is below certain threshold (ii) the maximum absolute deviation in the potential is less than the specified tolerance limit and (iii) the standard deviation in a density matrix element remains within a prescribed threshold. For

TABLE I: Variation of all the energy components and total number of electrons with respect to the grid parameters for Cl_2 along with the reference values at $R = 4.20$ a.u. All quantities are in a.u.

	$N_r = 32$		$N_r = 64$			$N_r = 128$		$N_r = 256$	Ref. [27]
Set	A	B	C	D	E	F	G	H	
h_r	0.3	0.4	0.2	0.3	0.4	0.1	0.2	0.1	
$\langle T \rangle$	11.00750	11.17919	11.18733	11.07195	11.06448	11.18701	11.07244	11.07244	11.07320
$\langle V_t^{ne} \rangle$	-83.43381	-83.68501	-83.70054	-83.45722	-83.44290	-83.69988	-83.45810	-83.45810	-83.45964
$\langle E_h \rangle$	37.94086	36.82427	36.83193	36.58714	36.57918	36.83133	36.58747	36.58747	
$\langle E_x \rangle$	-4.86173	-4.86641	-4.86778	-4.84360	-4.84245	-4.86771	-4.84374	-4.84373	
$\langle E_c \rangle$	-0.73575	-0.73521	-0.73530	-0.73374	-0.73366	-0.73530	-0.73374	-0.73374	
$\langle V_t^{ee} \rangle$	32.34338	31.22265	31.22885	31.00981	31.00306	31.22832	31.01000	31.01000	31.01078
$\langle E_{nu} \rangle$	11.66667	11.66667	11.66667	11.66667	11.66667	11.66667	11.66667	11.66667	11.66667
$\langle V \rangle$	-39.42376	-40.79570	-40.80503	-40.78074	-40.77317	-40.80489	-40.78144	-40.78144	-40.78219
$\langle E_{el} \rangle$	-40.08293	-41.28318	-41.28437	-41.37545	-41.37535	-41.28455	-41.37566	-41.37566	-41.37566
$\langle E \rangle$	-28.41626	-29.61651	-29.61770	-29.70878	-29.70868	-29.61789	-29.70900	-29.70900	-29.70899 ^a
N	13.89834	13.99939	13.99865	14.00002	14.00003	13.99864	14.00000	13.99999	13.99998

^aThis is from the grid-DFT calculation; the corresponding grid-free DFT value is -29.71530 a.u.

(ii) and (iii) 10^{-5} a.u. seemed appropriate while for (i), we used both 10^{-6} and 10^{-5} a.u. (see Section III).

III. RESULT AND DISCUSSION

At first, we examine the convergence and stability of our nonrelativistic ground state total energy as well as all the individual energy components for Cl_2 molecule with respect to the grid spacing h_r and number of grid points N_r ($r \in x, y, z$) at an internuclear distance 4.20 a.u. in Table I. We did a series of test calculations and here we present a select 8 of them. These are: (i) Sets A, B with $h_r = 0.3$ and 0.4 , both having $N_r = 32$; (ii) Sets C, D, E with $h_r = 0.2, 0.3, 0.4$, all having $N_r = 64$; (iii) Sets F, G with $h_r = 0.1, 0.2$, both having $N_r = 128$; and (iv) Set H with $h_r = 0.1$, $N_r = 256$. All the calculations in this table are performed with an energy convergence criterion of 10^{-7} a.u. The reference values denote the results obtained from the GAMESS suite of quantum chemistry program [27] with the same XC combination, basis set and effective core potential. The Hay-Wadt (HW) valence basis set [25, 26] is used for all the calculations done in this work, where the valence orbital is essentially split into inner and outer components (described by two and one primitive

gaussian functions respectively). Expectation values for the following energy operators are reported: kinetic energy $\langle T \rangle$, total nucleus-electron potential energy $\langle V_t^{ne} \rangle$, two-electron Coulomb repulsion energy $\langle E_H \rangle$, exchange energy $\langle E_X \rangle$, correlation energy $\langle E_C \rangle$, total two-electron potential energy $\langle V_t^{ee} \rangle$, nuclear repulsion energy $\langle E_{nu} \rangle$, total potential energy $\langle V \rangle$ ($\langle V_t^{ne} \rangle + \langle V_t^{ee} \rangle + \langle E_{nu} \rangle$), total electronic energy $\langle E_{el} \rangle$ and total energy $\langle E \rangle$ respectively. The Hartree, exchange and correlation energies of the reference values are not reported as these individual contributions were not available in the reference output. Furthermore, the total integrated electron density is given as N , which is a good measure of the quality of the results. We note that the reference values [27] for the total energy obtained from grid-DFT and grid-free DFT calculations are -29.70899 and -29.71530 a.u. respectively. The former uses the default “army grade” grid using Euler-MacLaurin quadratures for the radial integration and Gauss-Legendre quadrature for the angular integrations [11–13]. The grid-free calculations [19, 20] ideally use the resolution of identity to simplify the evaluation of molecular integrals over functionals, rather than the quadrature grids. The latter is quite appealing, for it enables one to avoid the finite grid and associated error; however this usually requires an extra *auxiliary* basis set to expand the identity. The first thing to note is that the maximum deviation in energy (off by almost 1.30 a.u.) from the reference value is shown by Set A; presumably the box length is insufficient to capture all the important contributions. This is also reflected in the poor value of N . As the spacing is increased to 0.4, the results for all the quantities get significantly better in Set B. As we further enlarge the box size with an increase in h_r to 0.5 a.u. (not shown in the table due to lack of space), the total energy reaches a value of -29.71012 a.u., which is lower than the reference value by 0.00113 a.u. This is a reasonable agreement with the reference value; however there may be slight caused by the combined effect of a large h_r and small N_r . It is noticed that Sets C and F both produce very similar results for all the quantities including N , as one expects intuitively, for they cover the same box length. Set B also corresponds to the same box size as the above two sets and indeed the total energy is again comparable; however the individual energy components and N show slight deviations. In Set D, our results for all the quantities including N are very nicely matching with the reference values. Keeping N_r fixed and increasing h_r to 0.4 a. u. in Set E, the total energy deviates by 0.00010 a.u. from Set D and N remains almost unchanged. Thus among A–E, Sets D, E are to be considered two best values. In order to gain further confidence and examine the variationality, several

TABLE II: Variation of all the energy components and total number of electrons with respect to the grid parameters for HCl along with the reference values at $R = 2.40$ a.u. All quantities are in a.u.

	$N_r = 32$	$N_r = 64$			$N_r = 128$		Ref. [27]
Set	B	C	D	E	F	G	
h_r	0.4	0.2	0.3	0.4	0.1	0.2	
$\langle T \rangle$	6.17590	6.17910	6.17900	6.17510	6.17909	6.17796	6.17811
$\langle V_t^{ne} \rangle$	-37.16617	-37.17230	-37.17252	-37.16470	-37.17228	-37.16998	-37.17042
$\langle E_h \rangle$	15.78969	15.79289	15.79266	15.78825	15.79287	15.77980	
$\langle E_x \rangle$	-2.74695	-2.74742	-2.74737	-2.74674	-2.74742	-2.73626	
$\langle E_c \rangle$	-0.41724	-0.41727	-0.41727	-0.41723	-0.41727	-0.41706	
$\langle V_t^{ee} \rangle$	12.62550	12.62820	12.62803	12.62428	12.62818	12.62648	12.62677
$\langle E_{nu} \rangle$	2.91667	2.91667	2.91667	2.91667	2.91667	2.91667	2.91667
$\langle V \rangle$	-21.62401	-21.62744	-21.62554	-21.62375	-21.62743	-21.62683	-21.62699
$\langle E_{el} \rangle$	-18.36478	-18.36501	-18.36551	-18.36532	-18.36501	-18.36554	-18.36555
$\langle E \rangle$	-15.44811	-15.44834	-15.44884	-15.44865	-15.44834	-15.44887	-15.44889 ^a
N	8.00023	7.99992	8.00002	8.00003	7.99992	8.00000	8.00003

^aThis is from the grid-DFT calculation; the corresponding grid-free DFT value is -15.44888 a.u.

extra calculations (Sets F, G and H) are done in a relatively larger and finer mesh. Thus Sets E, G, H all correspond to the same box length of 25.6 a.u. However, from E to G, total energy changes by only 0.00032 a.u., while G and H Set results are virtually identical. It is quite gratifying that Set G and H results not only *completely* match with each other in total energy; the component energies are identical up to 5th decimal place. It may also be mentioned that a calculation for $N_r = 128, h_r = 0.3$ (Set I) (not shown in the table) leads to an energy value of -29.70909 a.u., which again exactly coincides with Sets G and H. On the basis of above discussion, it is abundantly clear that Sets D, E, G, H are our four best results; while Sets D, E are sufficiently accurate for all practical purposes.

Next in Table II we report results for the heteronuclear diatomic, HCl. Our basic presentation strategy remains the same as in Table I, although in this case a fewer number of grid sets are given. Thus a total of 6 sets B–G are presented. As in Table I, here also we used an energy convergence criterion of 10^{-6} a.u. The reference total energies from the respective grid and grid-free calculations of -15.44889 and -15.44888 a.u. seem to be in a better agreement with each other than that for Cl_2 . Overall, very similar trend is observed in this case as the grid parameters are changed, as for Cl_2 . Note that Set B was inadequate for Cl_2 ; but for HCl this seems quite reasonable. All of these sets are capable of reproducing

TABLE III: Comparison of the calculated eigenvalues of Cl_2 and HCl with the reference values (grid-DFT). Negative values are given in a.u.

MO	$\text{Cl}_2(R=4.2 \text{ a.u.})$						MO	$\text{HCl}(R=2.4 \text{ a.u.})$					
Set	D	E	G	I	H	Ref. [27]		B	C	D	F	G	Ref. [27]
$2\sigma_g$	0.8266	0.8274	0.8268	0.8268	0.8268	0.8267	2σ	0.7788	0.7784	0.7787	0.7784	0.7786	0.7786
$2\sigma_u$	0.7167	0.7175	0.7168	0.7169	0.7168	0.7168	3σ	0.4228	0.4225	0.4230	0.4226	0.4228	0.4228
$3\sigma_g$	0.4332	0.4340	0.4334	0.4334	0.4334	0.4333	$1\pi_x$	0.2862	0.2861	0.2866	0.2861	0.2864	0.2864
$1\pi_{xu}$	0.3515	0.3517	0.3516	0.3517	0.3516	0.3516	$1\pi_y$	0.2862	0.2861	0.2866	0.2861	0.2864	0.2864
$1\pi_{yu}$	0.3515	0.3517	0.3516	0.3517	0.3516	0.3516							
$1\pi_{xg}$	0.2859	0.2861	0.2861	0.2861	0.2861	0.2860							
$1\pi_{yg}$	0.2859	0.2861	0.2861	0.2861	0.2861	0.2860							

the reference values nicely up to the third place of decimal, although Set B result is, to some extent, inferior to the other five sets in terms of the individual energy components and N . All the energies, however, are above the reference value. Just as in previous table, a gradual improvement is observed as one passes from Set B–C–D. Moreover, Sets C and F results show mutual agreement with each other as in Table I. However for Cl_2 , their total energies were above the reference value by roughly 0.091 a.u. and N was correct only up to second decimal-place; for HCl , on the other hand, these are above the reference value by only 0.00055 a.u. and N shows fourth place of decimal accuracy. As one passes from Set D to E, N remains almost unchanged and total energy increases by approximately 0.0002 a.u. (a trend also observed for Cl_2). Further calculations with $N_r = 128$, $h_r = 0.3$ (Set I), produces exactly identical result as in Set G expectedly, and are thus not presented separately. Not surprisingly, as in Cl_2 , in this case also our three best results are those from Sets D, E and G; with the former two being sufficiently accurate for all purposes, once again.

Table III lists the computed eigenvalues for several sets for Cl_2 and HCl at the respective R values as in Tables I and II, along with the reference values. For Cl_2 , the calculated eigenvalues are either completely matching or show an absolute maximum deviation of only 0.0001 a.u. for the Sets D, G, I and H; Set E gives an absolute maximum deviation of 0.0007 a.u. (for $2\sigma_g$, $2\sigma_u$ and $3\sigma_g$). This is also apparent from a consideration of their performances in Table I. For HCl , Sets B, D, F give an absolute maximum deviation of 0.0002 a.u., while the same for Set C is 0.0003 a.u. Set G results completely match with the reference eigenvalues.

For further examination, Table IV displays the calculated negative total energies of Cl_2

TABLE IV: Comparison of the calculated potential energy curve of Cl_2 and HCl for several grid parameters along with the reference values (grid-DFT). Negative values are given in a.u.

R (a.u.)	Cl ₂ (Total energy relative to -29 a.u.)					R(a.u.)	HCl(Total energy relative to -15 a.u.)			
Set	D	E	G	I	Ref. [27]		B	C	D	Ref. [27]
3.50	0.6508	0.6504	0.6509	0.6508	0.6509	1.60	0.1327	0.1329	0.1330	0.1331
3.60	0.6697	0.6694	0.6698	0.6697	0.6698	1.70	0.2293	0.2294	0.2296	0.2297
3.70	0.6839	0.6836	0.6840	0.6839	0.6840	1.80	0.3004	0.3005	0.3007	0.3008
3.80	0.6943	0.6940	0.6944	0.6943	0.6944	1.90	0.3520	0.3523	0.3525	0.3526
3.90	0.7014	0.7012	0.7015	0.7015	0.7015	2.00	0.3890	0.3893	0.3895	0.3896
4.00	0.7059	0.7057	0.7061	0.7060	0.7060	2.10	0.4147	0.4150	0.4152	0.4153
4.10	0.7082	0.7080	0.7084	0.7083	0.7084	2.20	0.4317	0.4321	0.4324	0.4325
4.20	0.7088	0.7086	0.7090	0.7089	0.7090	2.30	0.4420	0.4425	0.4430	0.4432
4.30	0.7079	0.7077	0.7082	0.7081	0.7081	2.40	0.4481	0.4483	0.4488	0.4489
4.40	0.7059	0.7057	0.7062	0.7061	0.7062	2.50	0.4501	0.4505	0.4508	0.4509
4.50	0.7030	0.7029	0.7033	0.7032	0.7033	2.60	0.4494	0.4498	0.4501	0.4502
4.60	0.6994	0.6993	0.6997	0.6996	0.6997	2.70	0.4466	0.4472	0.4473	0.4474
4.70	0.6952	0.6953	0.6956	0.6955	0.6956	2.80	0.4427	0.4429	0.4431	0.4431
4.80	0.6906	0.6908	0.6911	0.6910	0.6911	2.90	0.4369	0.4375	0.4378	0.4378
4.90	0.6858	0.6861	0.6864	0.6863	0.6864	3.00	0.4303	0.4310	0.4316	0.4317
5.00	0.6809	0.6812	0.6816	0.6815	0.6816	3.10	0.4243	0.4249	0.4251	0.4251

(relative to -29 a.u.) for Sets D, E, G and I ($N_r = 128, h_r = 0.3$) in columns 2–5 with the reference values (column 6) covering a broad bond length region of 3.50–5.00 a.u. In the right panel, the same for HCl is given for three Sets B, C, D along with those obtained from the reference calculations (all relative to -15 a.u.) for $R = 1.60 - 3.10$ a.u., in columns 8–11. These are depicted in Fig. 1 for smaller R ranges to show the energy changes more clearly. We note that all these calculations are performed with a less stricter energy convergence criterion of 10^{-5} a.u. For Cl_2 , all these four sets reproduce the qualitative shape of the potential energy curve very well for the entire range. Set D produces energy values quite well (higher by only 0.0001 a.u.) until $R = 4.00$ a.u., and thereafter develops a gradual tendency to deviate more. Nevertheless the maximum deviation is quite small (only 0.0007 a.u.), that occurs for $R = 5.00$. The other two sets G and I are either completely matching with the reference values or show an absolute maximum deviation of 0.0001 a.u. We also note that the computed energy values have always remained above the reference values except for two instances ($R = 4.00$ and 4.30 for Set G). And leaving aside these two R values, Set G shows exact quantitative agreement with the reference curve. For HCl also, the three sets give very good qualitative agreement for the whole range of R as seen from their nearly

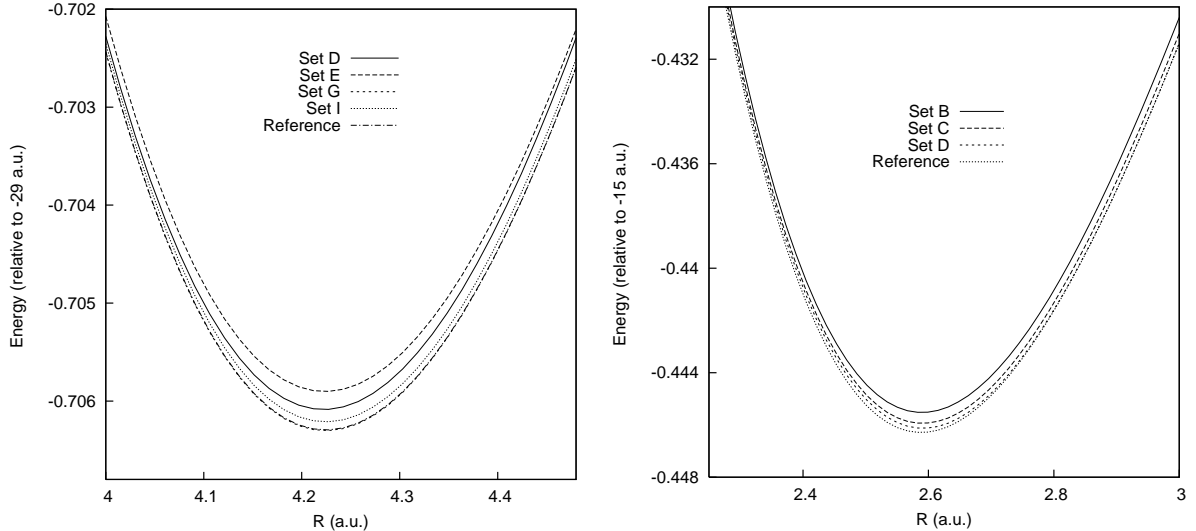


FIG. 1: Potential energy curves for Cl_2 (left panel) and HCl (right panel) for different grid parameters.

identical shapes. The absolute maximum discrepancies for the three sets B, C, D are 0.0014, 0.0007 and 0.0002 for $R = 3.00$, 2.30 and 2.30 a.u. respectively. The best matching is observed with Set D. Obviously, as demonstrated for Cl_2 case, even more accurate results could be obtained with a fine-tuning of the grid parameters and refining the convergence criteria.

Once the stability and reliability of our calculation is established, now Table V gives the computed kinetic, potential and total energies as well as N for selected 10 molecules and 3 atoms (HCl and Cl_2 are omitted as they have been discussed earlier) to judge its applicability for a larger set of chemical systems. These are ordered in terms of increasing N ; corresponding grid-DFT [27] values are quoted for comparison. All these calculations in this table are performed using grid Set E, which was found to be quite satisfactory for HCl and Cl_2 . However, it may be mentioned that, for all these systems, using a smaller grid with $N_r = 32$, $h_r = 0.5$, we obtained converged results of correspondingly similar accuracy as for Cl_2 (see discussion on Table I). For all of these species, we see there is excellent agreement with the reference values for all the quantities. In several occasions, energies are identical as the reference (for example As, Br_2). The maximum deviation is observed for Na_2Cl_2 (by 0.00056 a.u.). This once again demonstrates the faithfulness of the present results.

Finally in Table VI, to gain further confidence, the calculated ionization energies, $-\epsilon_{\text{HOMO}}$ (in a.u.) are compared with the grid-DFT result [27]; atomization energies are *also* compared

TABLE V: Kinetic ($\langle T \rangle$), potential ($\langle V \rangle$), total (E) energies and N for several molecules and atoms. All quantities in a.u. PW=Present Work.

System	$\langle T \rangle$		$-\langle V \rangle$		$-\langle E \rangle$		N	
	PW	Ref. [27]	PW	Ref. [27]	PW	Ref. [27]	PW	Ref. [27]
Na ₂	0.14507	0.14499	0.52800	0.52791	0.38292	0.38292	1.99999	2.00000
NaH	0.56931	0.56912	1.29712	1.29697	0.72781	0.72785	1.99999	2.00005
P	2.35430	2.35334	8.73501	8.73404	6.38070	6.38071	5.00000	4.99999
As	2.07461	2.07354	8.10154	8.10047	6.02693	6.02693	5.00000	4.99999
Br	4.22038	4.22011	17.28157	17.28131	13.06119	13.06120	7.00000	6.99967
NaCl	5.77569	5.77639	20.92133	20.92235	15.14564	15.14596	8.00001	8.00059
H ₂ S	4.90204	4.90197	16.10707	16.10698	11.20503	11.20501	8.00000	7.99989
PH ₃	4.08953	4.08953	12.27387	12.27383	8.18434	8.18430	8.00000	7.99965
Br ₂	8.55754	8.55716	34.74793	34.74755	29.19039	29.19039	14.00000	14.00003
H ₂ S ₂	8.75379	8.75342	30.00250	30.00213	21.24872	21.24871	13.99999	13.99996
MgCl ₂	11.62114	11.62208	42.34513	42.34621	30.72399	30.72413	16.00004	15.99957
Na ₂ Cl ₂	11.55066	11.55242	41.92870	41.92990	30.37804	30.37748	16.00002	15.99686
SiH ₂ Cl ₂	13.95036	13.94989	48.78729	48.78685	34.83693	34.83696	19.99999	20.00015

with the experimental results [32] besides grid-DFT of [27] and other DFT results [33, 34]. Our computed results for both these quantities are in excellent agreement with those of [27]. However, the atomization energies in several occasions show substantial discrepancy from experimental values and other DFT results. Note that the experimental values include zero-point vibrational corrections as well as relativistic effects. The largest error is found for Cl₂ (about 13.5 kcal/mole). The results of [33, 34] are based on all-electron calculations. Former used the 6-311++G(d,p) basis set and employed a combination of approximate exchange SC- α (recovering all the behavior of exact exchange) and a scaled GGA correlation functional. The latter used an optimum GGA/exact-exchange DFT. Probably use of more appropriate basis set and better XC functionals would further improve the present results.

A few remarks may be made before passing. In this work our primary motivation was to demonstrate that the real-space CCG coupled with the Fourier convolution technique as employed here for the Hartree potential, could deliver accurate, physically meaningful results of “chemical” accuracy for molecular systems, through a small representative sets of 12 molecules and 3 atoms. Thus no effort was made to reproduce either the most accurate theoretical results or the experimental values, which may be considered in future. These would inevitably require the inclusion of more extended and elaborate basis sets (containing the polarized and diffuse functions) as well as more accurate and sophisticated nonlocal XC

TABLE VI: Highest occupied molecular orbital energy, $-\epsilon_{\text{HOMO}}(\text{a.u.})$ and atomization energies (kcal/mole) for molecules. PW=Present Work.

System	$-\epsilon_{\text{HOMO}}(\text{a.u.})$		Atomization energy(kcal/mol)			
	PW	Ref. [27]	PW	Ref. [27]	Other DFT	Expt. [32]
Na ₂	0.1050	0.1051	14.64	14.64	16.15 ^a ,22.1 ^b	17.0
NaH	0.1458	0.1457	47.17	47.17		47.2
HCl	0.2863	0.2864	104.16	104.16	98.38 ^a ,101.6 ^b	102.2
NaCl	0.1811	0.1810	97.62	97.63	88.18 ^a ,96.3 ^b	97.4
H ₂ S	0.2267	0.2265	178.65	178.65	172.5 ^b	173.2
PH ₃	0.2323	0.2323	241.56	241.55	227.14 ^a ,227.1 ^b	227.1
Cl ₂	0.2861	0.2860	43.72	43.73	40.18 ^a ,59.0 ^b	57.2
Br ₂	0.2542	0.2540	42.68	42.68		45.4
H ₂ S ₂	0.2371	0.2370	222.03	222.04		229.6
MgCl ₂	0.2803	0.2805	185.14	185.14		187.4
Na ₂ Cl ₂	0.2126	0.2125	248.33	248.34		243.1
SiH ₂ Cl ₂	0.2903	0.2905	337.55	337.55		341.8

^aRef. [33].

^bRef. [34].

functionals (with gradient and Laplacian corrections) having correct short- and long-range properties. At this stage, a few words on scaling is in order. Denoting N_b and N_g as the number of grid points and basis functions respectively, one can assign the following scaling relations to the four most important steps of the whole process: (a) construction of the localized basis set scales as N_g , (b) generation of the basis function in the grid scales as $N_b N_g$, (c) calculation of the electron density in the grid scales as $N_b^2 N_g$, and finally (d) build-up of the one- and two-body matrix elements of the Fock matrix scales as N_b^2 and $N_b^2 N_g$ respectively. More detailed analysis of the scaling and computational time with respect to the system size may be considered in future communications. It is worthwhile mentioning that our main motivation in this work is to build up a stable platform which enables us to perform the real-time dynamics studies (such as multi-photon ionization, high-order harmonic generation, etc.) of polyatomics in presence of an intense laser field that utilizes and exploits the enormous advances made in LCAO-GTO-based molecular DFT approaches over the years through many pioneering works. In taking up that, it was felt that TD implementation of the overwhelmingly successful ACG-based codes could be quite complicated and CCG-based approaches might be easier and straightforward to handle without making serious compromise on the accuracy and reliability. Thus the purpose is not to develop

another electronic structure code when there are several highly elegant and versatile quantum chemistry packages are available; but to make a modest base which provides sufficient accuracy and reliability to pursue the dynamical calculations, as mentioned. Although one could envisage some inaccuracies associated with the direct numerical integrations on the grid (due to the incompleteness of the grid), as our results suggest, with a proper adjustment of the grid parameters, this may not be so detrimental, at least for the systems of this work and use of non-uniform variable or adaptive grids may partly alleviate this problem. We note that we have also made some test calculations for systems like P_4 , S_8 (to be presented elsewhere), etc., leading to similar kind of results as the present work. This further validates the significance of this work.

IV. FUTURE AND OUTLOOK

We presented a detailed study on the performance of CCG in the context of atomic and molecular DFT calculations. The viability and feasibility of this is demonstrated by applying it to a set of 12 molecules and 3 atoms. This was achieved through an accurate representation of the classical Hartree potential through a Fourier convolution method on the real grid. Core electrons were represented by the HW pseudopotential and local LDA XC potentials were employed. An analysis on a cross-section of the calculated quantities including energy components, eigenvalues, ionization energies, atomization energies, as well as the potential energy curves, reveal that this can offer fairly accurate and reliable results. The results are variationally well-founded. More elaborate and systematic investigation on the properties such as atomization energies, vibrational properties, reaction energies, etc., of different chemical systems like small clusters, weakly-bonded molecules would be required to assess the success and performance of this approach. Better basis sets and XC functionals would be needed for further improvement. It may be interesting to study the performance of this in the context of all-electron calculations. Other interesting areas of study would constitute the real-time dynamics of small to medium size molecules in presence of a strong external TD field, or the chemical descriptor analysis through various local and global quantities (like softness, hardness, fukui function, etc). Some of these issues are currently being investigated by us.

Acknowledgments

I am grateful to Prof. D. Neuhauser for his generous support, encouragement and useful discussion throughout the course of this work. A special thank goes to Dr. E. I. Proynov for numerous valuable, constructive comments and a critical reading of the manuscript. I am thankful to Professors B. M. Deb, S. I. Chu, K. D. Sen and A. J. Thakkar for fruitful discussions. It is a pleasure to thank Drs. Z. Zhou and R. Baer for their comments. The anonymous referee is thanked for valuable and constructive suggestions. The warm hospitality provided by the Univ. of California, Los Angeles, is gratefully acknowledged.

- [1] P. Hohenberg and W. Kohn, Phys. Rev. B **136**, 864 (1964).
- [2] W. Kohn and L. J. Sham, Phys. Rev. A **140**, 1133 (1965).
- [3] J. R. Chelikowsky, N. Troullier, K. Wu and Y. Saad, Phys. Rev. B **50**, 11355 (1994).
- [4] J. Andzelm, E. Radzio and D. R. Salahub, J. Chem. Phys. **83**, 4573 (1985).
- [5] J. Andzelm and E. Wimmer, J. Chem. Phys. **96**, 1280 (1992).
- [6] G. Lippert, J. Hutter and M. Parinello, Theor. Chem. Acc. **103**, 124 (1999).
- [7] M. Krack and M. Parinello, Phys. Chem. Chem. Phys. **2**, 2105 (2000).
- [8] A. D. Becke, J. Chem. Phys. **88**, 2547 (1988).
- [9] O. Treutler and R. Ahlrichs, J. Chem. Phys. **102**, 346 (1995).
- [10] M. M. Mura and P. J. Knowles, J. Chem. Phys. **104**, 9848 (1996).
- [11] C. W. Murray, N. C. Handy and G. J. Laming, Mol. Phys. **78**, 997 (1993).
- [12] P. M. W. Gill, B. G. Johnson and J. A. Pople, Chem. Phys. Lett. **209**, 506 (1993).
- [13] R. Lindh, P. -A. Malmqvist and L. Gagliardi, Theor. Chem. Acc. **106**, 178 (2001).
- [14] V. I. Lebedev, Zh. Vychisl. Mat. Mat. Fiz. **15**, 48 (1975); *ibid.* **16**, 293 (1976).
- [15] M. Krack and A. M. Köster, J. Chem. Phys. **108**, 3226 (1998).
- [16] L. Füsti-Molnár and P. Pulay, J. Chem. Phys. **7827**, (2002).
- [17] J. Kong, S. T. Brown, L. Füsti-Molnár, J. Chem. Phys. **124**, 094109 (2006).
- [18] S. T. Brown, L. Füsti-Molnár and J. Kong, Chem. Phys. Lett. **418**, 490 (2006).
- [19] Y. C. Zheng and J. Almlöf, Chem. Phys. Lett. **214**, 397 (1993).
- [20] K. R. Glaesemann and M. S. Gordon, J. Chem. Phys. **108**, 9959 (1998).

- [21] G. C. Martyna and M. E. Tuckerman, J. Chem. Phys. **110**, 2810 (1999).
- [22] P. Minary, M. E. Tuckerman, K. A. Pihakari and G. J. Martyna, J. Chem. Phys. **116**, 5351 (2002).
- [23] S. Obara and A. Saika, J. Chem. Phys. **84**, 3963 (1986).
- [24] L. E. McMurchie and E. R. Davidson, J. Comput. Phys. **26**, 218 (1978).
- [25] W. R. Wadt and P. J. Hay, J. Chem. Phys. **82**, 284 (1985).
- [26] P. J. Hay and W. R. Wadt, J. Chem. Phys. **82**, 299 (1985).
- [27] M. W. Schmidt, K. K. Baldridge, J. A. Boatz, S. T. Elbert, M. S. Gordon, J. H. Hensen, S. Koseki, N. Matsunaga, K. A. Nguyen, S. J. Su, T. L. Windus, M. Dupuis and J. A. Montgomery, J. Comput. Chem. **14**, 1347 (1993).
- [28] T. L. Beck, Rev. Mod. Phys. **72**, 1041 (2000).
- [29] S. H. Vosko, L. Wilk and M. Nusair, Can. J. Phys. **58**, 1200 (1980).
- [30] H. Sambe and R. H. Felton, J. Chem. Phys. **62**, 1122 (1975).
- [31] B. I. Dunlap, J. W. D. Connolly and J. R. Sabin, J. Chem. Phys. **71**, 3396 (1979); *ibid.* **71**, 4993 (1979).
- [32] H. Y. Afeefy, J. E. Liebman and S. E. Stein, “Neutral Thermochemical Data” in *NIST Chemistry WebBook, NIST Standard Reference Database Number 69*, Eds. P. J. Linstrom and W. G. Mallard, June 2005, National Institute of Standards and Technology, Gaithersburg MD, 20899 (<http://webbook.nist.gov>).
- [33] M. Cafiero, Chem. Phys. Lett. **418**, 126 (2006).
- [34] A. D. Becke, J. Chem. Phys. **107**, 8554 (1997).